



Oxidative stress exacerbates dextran sulfate sodium-induced ulcerative colitis in ICR mice

Nitima Tatiya-aphiradee^{1,2} · Waranya Chatuphonprasert^{2,3} · Kanokwan Jarukamjorn^{1,2}

Received: 21 December 2019 / Accepted: 20 May 2020 / Published online: 3 June 2020
© Institute of Molecular Biology, Slovak Academy of Sciences 2020

Abstract

Ulcerative colitis (UC) is a complex, multifactorial disorder which can be aggravated by oxidative stress. Dextran sulfate sodium (DSS)-induced UC in inbred mice is the most commonly used animal-model. However, these populations lack genetic variability therefore this study aimed to establish a DSS-induced UC model in outbred ICR mice and to assess its association with the oxidant-antioxidant system. Male ICR mice were administered a 40 kDa-DSS solution (6 g/kg/day; 0.25 mL 21% DSS 4 times per day) intragastrically for 4 and 7 consecutive days (n = 5). Disease activity index (DAI) was determined daily from body weight and stool characteristics. At the end of the study, colons were collected to examine histology, myeloperoxidase activity, and expression of superoxide dismutase 1 and 2 (*Sod1* and *Sod2*) and catalase (*Cat*). DSS-treated mice demonstrated daily increases in DAI score with significantly shortened colons, an indirect marker of inflammation in UC. Histological examination of DSS-treated colons revealed goblet cell loss, crypt damage, and epithelial erosion, followed by infiltration of mast cells to the mucosa with mucin depletion. Myeloperoxidase activity was elevated in the DSS-treated mice while *Sod1*, *Sod2*, and *Cat* were suppressed compared to controls. A DSS-induced UC model was established in ICR mice with associated oxidative stress triggering. This outbred-mouse model could prove useful for investigating the underlying pathophysiological mechanisms of UC in terms of oxidant-antioxidant balance.

Keywords Catalase · Dextran sulfate sodium · Disease activity index · Outbred mouse strain · Superoxide dismutase · Ulcerative colitis

Abbreviations

CAT	catalase
DSS	dextran sulfate sodium
DAI	disease activity index
IBD	inflammatory bowel disease
MPO	myeloperoxidas
ROS	reactive oxygen species
SOD	superoxide dismutase
UC	ulcerative colitis

Introduction

Ulcerative colitis (UC) is a subcategory of inflammatory bowel disease (IBD). It is a disorder in the gastrointestinal system affecting the caecum, colon, and rectum usually in a continuous pattern (Baumgart and Sandborn 2007) and characteristically affecting the mucosal surface of the colon. The lesion initiates in the rectum and extends proximally through the colon. Symptoms of UC are often insidious with gradual onset. Although the precise etiology of UC remains unclear, it is generally hypothesized to be a multifactorial combination of genetic, environmental, and gut microbiota effects which trigger inflammatory and immune responses in the luminal mucosa (Ordás et al. 2012). Several conditions such as viral and bacterial infection, certain types of food, and stress can exacerbate UC (Singh et al. 2009).

Oxidative stress is one significant factor associated with the pathophysiology of UC (Balmus et al. 2016) and the overproduction of reactive oxygen species (ROS) has been reported to provoke intestinal inflammation (Halliwell 1997). Imbalance

✉ Kanokwan Jarukamjorn
kanok_ja@kku.ac.th

¹ Faculty of Pharmaceutical Sciences, Khon Kaen University, Mitraparb road, Khon Kaen 40002, Thailand

² Research Group for Pharmaceutical Activities of Natural Products using Pharmaceutical Biotechnology (PANPB), Khon Kaen University, 40002 Khon Kaen, Thailand

³ Faculty of Medicine, Mahasarakham University, Mahasarakham 44000, Thailand

of ROS production and antioxidant capacity leading to oxidative stress is implicated in several human disorders including UC (Halliwell 1997). Hence, the investigation of antioxidant activity could illuminate our understanding of UC mechanisms.

Over more than 20 years, a murine UC model has been used to study the mechanisms of the disease. The animal model has come to be recognized as an indispensable tool to examine the underlying pathophysiological mechanisms and to improve medical therapy. Among the various techniques of UC induction, the chemical-induced UC model, particularly dextran sulfate sodium (DSS)-induced UC model, is the most widely employed and well established (Perše and Cerar 2012) due to its simplicity and reproducibility and characteristic features similar to UC in human patients (Cheon et al. 2006; Hirata et al. 2007). Genetic background plays a significant role in DSS-induced UC in mice (Perše and Cerar 2012) via the regulation of inflammatory responses (Perše and Cerar 2012; Xavier and Podolsky 2007). While several studies have shown inbred mouse strains are susceptible to DSS-induced UC and develop severe lesions (Barone et al. 2018; Mahler et al. 1998; Stevceva et al. 1999), studies of DSS-induced UC in outbred mouse strains, particularly with regard to the oxidant-antioxidant response, are limited (Kim et al. 2010). Institute of Cancer Research (ICR) mice are an outbred strain that has been extensively utilized in diverse medical research fields such as pharmacology, oncology, and toxicology (Kim et al. 2017). Therefore, since human populations have high genetic variability (Frazer et al. 2009), the present study aimed to establish and characterize a DSS-induced UC model in ICR mice.

Materials and methods

Animals

Twenty male ICR mice (5-week-old) were supplied by the Northeast Laboratory Animal Center, Khon Kaen University, Khon Kaen, Thailand. All mice were housed in stainless steel cages with corn cob bedding and were maintained under a 12 h light/dark cycle with controlled humidity ($45 \pm 2\%$) at 25°C in the animal laboratory unit, Faculty of Pharmaceutical Sciences, Khon Kaen University, under the supervision of a certified laboratory veterinarian. Commercial regular diet and water were supplied *ad libitum*. All animals were acclimated for one week before the start of treatment. The animal handling and treatment protocol was approved by the Animal Ethic Committee of Khon Kaen University (IACUC-KKU-26/61) following the Declaration of Helsinki with the Guide for the Care and Use of Laboratory Animals as adopted and promulgated by the United States National Institutes of Health.

Induction of UC

The mice were divided into 4 groups ($n = 5$ each). An aqueous solution of 21% (w/v) DSS (40 kDa; Sigma-Aldrich Chemicals, St. Louis, Missouri, USA) was prepared. The mice were administered a 0.25 mL-aliquot of the DSS solution by a gastric lavage-tube 4 times per day (6 g/kg/day) for either 4 or 7 consecutive days. The control groups were given sterile water.

Evaluation of disease activity index (DAI)

Each mouse was placed into a cage without bedding for 15 min to examine the stool characteristics (Chassaing et al. 2014). Body weight, stool consistency, and presence of blood in stool were recorded daily. Changes in these factors were scored to determine DAI. Scores were given for body weight loss (0, no reduction in body weight; 1, 1–5%; 2, 6–10%; 3, 11–20%; and 4, > 20%), reduced stool consistency (0, normal; 1, slightly loose stools; 2, loose stools; 3, diarrhea; 4, watery diarrhea), and bleeding in stools (0, normal; 2, slight bleeding; 4, gross bleeding) (Xiao et al. 2013). The total DAI scores ranged from 0 to 12. On the last day of the experiment (day 4 or day 7), all mice were euthanized, and the colons were collected to measure the length from the ileocecal junction to the anal verge for evaluation of indirect inflammation (Xiao et al. 2013) before further examination.

Histological examination

The proximal colon was placed in a tissue cassette after washing with phosphate buffer saline ($1 \times \text{PBS}$). The tissue was soaked in cold 10% neutral-buffered formaldehyde overnight, followed by serial dehydration from 50 to 100% ethanol. After that, the tissue was embedded in paraffin and cut into 5- μm sections using a microtome (HM315R, Microm, South Carolina, US) prior to placing onto a microscopic slide for hematoxylin and eosin (H&E; Bio-Optica, Milano, Italy) staining. Histological structures were assessed and scored as previously described (Tamaki et al. 2006). Each colon was scored according to: the severity of inflammation (0, none; 1, mild; 2, moderate; 3, severe), the extent of inflammation (0, none; 1, mucosa; 2, mucosa and submucosa; 3, transmural), and the amount of crypt damage (0, none; 1, 1/3 damaged; 2, 2/3 damaged; 3, crypts lost but epithelial surface present; 4, crypts and epithelial surface lost). The histological score was calculated by summing these three parameters with a maximum total score of 10. Sections were also stained with toluidine blue (Sigma-Aldrich Chemicals) and alcian blue (Sigma-Aldrich Chemicals) to observe mast cell infiltration and goblet cell loss, respectively. All slides were examined using an inverted microscope (Motic[®] AE2000,

Kowloon, Hong Kong) coupled with the Motic® image plus 3.0 software.

Determination of myeloperoxidase (MPO) activity

Middle colon homogenate was centrifuged at $19,000 \times g$ at 4°C for 15 min. A $7 \mu\text{L}$ -aliquot of supernatant was mixed with $200 \mu\text{L}$ of a mixture of 0.5 M hydrogen peroxide (Fisher Scientific, Leicestershire, UK) and 0.167 mg/mL *O*-dianisidine dihydrochloride (Sigma-Aldrich Chemicals) (1:2,000) in a 96-well plate. The absorbance of the reaction mixture was measured at a wavelength of 450 nm at 60 s-intervals for 30 min. The MPO activity was calculated by comparing to standard MPO and reported as unit/mg protein (Kim et al. 2012). The protein content was determined by the Bradford method using bovine serum albumin as the standard (Bradford 1976).

Total RNA extraction and quantitative determination of mRNA expression by RT/ real time PCR

Total RNA was extracted from the proximal colon using the guanidine thiocyanate-phenol-chloroform method (Jarukamjorn et al. 1999). The total RNA concentration was determined using a UV-Vis spectrophotometer (Nanodrop 2000C, Thermo Scientific, New York, US). RNA integrity was examined by Novel juice® (GeneDireX, Tai Chung, Taiwan) stained 1.25% agarose gel electrophoresis prior to converting to cDNA using ReverTraAce® (Toyobo, Osaka, Japan) under the thermal program recommended by the supplier: 25°C for 10 min, 42°C for 60 min, and 95°C for 5 min. The expression of superoxide dismutase 1 and 2 (*Sod1* and *Sod2*) and catalase (*Cat*) mRNA was analyzed using a real time PCR thermal cycler (CFX96, Bio-Rad®, California, USA) with specific primers which were designed using Primer-BLAST (<https://www.ncbi.nlm.nih.gov/tools/primer-blast/>) and synthesized by Bio Basic, Inc. (Markham, Ontario, Canada). The primers were as follows: *Sod1*, forward 5'-AAG GCC GTG TGC GTG CTG AA-3' and reverse 5'-CAG GTC TCC AAC ATG CCT CT-3' (Jarukamjorn et al. 2019); *Sod2*, forward 5'- GCA CAT TAA CGC GCA GAT CA-3' and reverse 5'-AGC CTC CAG CAA CTC TCC TT-3' (Jarukamjorn et al. 2019); *Cat*, forward 5'-GCA GAT ACC TGT GAA CTG TC-3' and reverse 5'-GTA GAA TGT CCG CAC CTG AG-3' (Jarukamjorn et al. 2019); *Gapdh*, forward 5'-CCT CGT CCC GTA GAC AAA A-3' and reverse 5'-TGA AGG GGT CGT TGA TGG C-3' (Tatiya-aphiradee et al. 2019). The mRNA level of each gene was normalized to that of a reference *Gapdh* gene.

Statistical analysis

The DAI and histological scores are expressed as mean \pm SEM; other data are expressed as mean \pm SD before analysis by the Student's *t*-test using the SPSS statistical program version 22.00. *p*-value < 0.05 was considered significant.

Results

Effect of DSS on the disease activity index (DAI)

The severity of the disease was indicated by the DAI score (Xiao et al. 2013). The DSS induced mice demonstrated a daily increase in DAI score compared to the controls after both 4 (Fig. 1a) and 7 days (Fig. 1b). Furthermore, after 4 and 7 days of induction, the colons were significantly shortened (Fig. 1c, d, e). This parameter was classified as an indirect marker of inflammation. Severe diarrhea and hematochezia were found after prolonged exposure to DSS for 7 days (Fig. 1e).

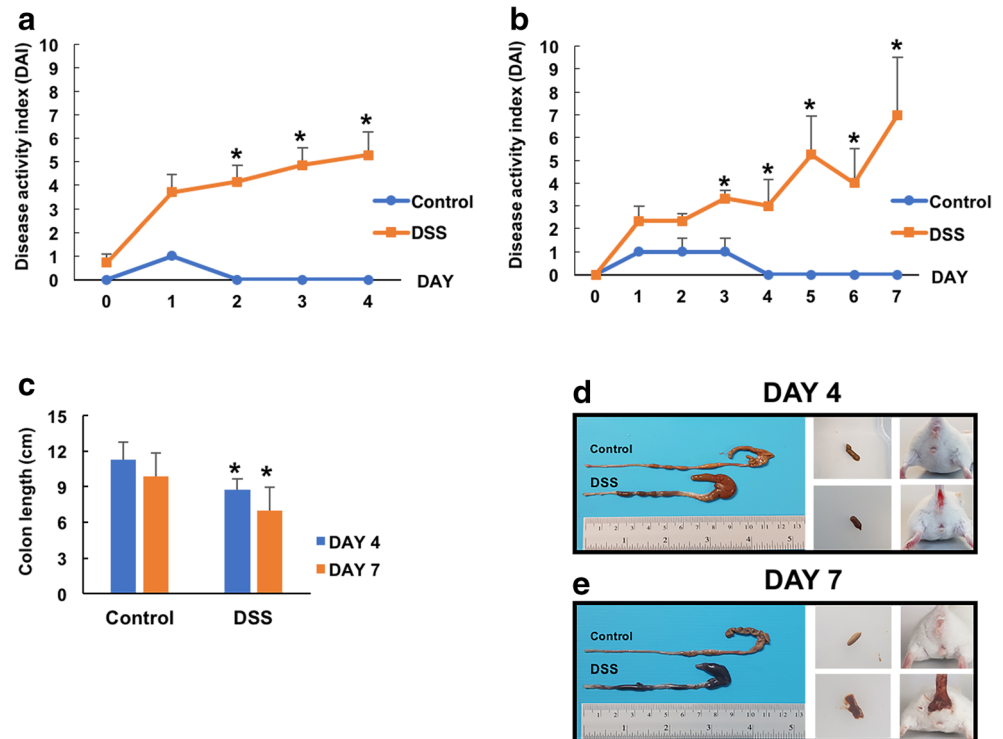
Effect of DSS on colon morphology

DSS induction resulted in damage to the colon. On day 4, DSS-treated mice exhibited histological changes including goblet cell (GC) depletion, damage to the crypt of Lieberkühn (CL), and epithelial erosion (square) (Fig. 2a). Moreover, DSS treatment promoted infiltration of inflammatory cells (red arrows) to the mucosa layer. Controls presented with undamaged crypts in the mucosal layer, no goblet cell loss, and no inflammatory cell infiltration. Interestingly, on day 7 of induction, the crypt structure was highly irregular and goblet cells had disappeared (Fig. 2b). This was accompanied by increased inflammatory cell infiltration and followed by severe epithelial erosion and ulceration. The histological scores of the DSS-treated mice were significantly higher than those of the controls at both day 4 and day 7 of induction (Fig. 2c). DSS triggered an infiltration of mast cells (black arrows) in the mucosal layer of the colon at both day 4 (Fig. 3a) and day 7 (Fig. 3b). While the cavities of crypts in the control mice were filled with mucin (black arrows) secreted by goblet cells (Fig. 4), the DSS-treated mice demonstrated mucin depletion at 4 days (Fig. 4a) and disappearance at 7 days (Fig. 4b).

Effect of DSS on myeloperoxidase activity in the colon

DSS resulted in a significant increase in MPO activity in the colon after both 4 and 7 days of induction, although prolonged induction for 7 days resulted in a more extensive decline in MPO activity (Fig. 5).

Fig. 1 Effects of DSS on disease activity index (DAI), colon length, and macroscopic changes of the colon in ICR mice. **a** DAI on day 4 and **b** DAI on day 7. DAI 0 represents no symptoms of the disease: no change in body weight, stool consistency, or presence of blood in stool and DAI 10 represents the most severe symptoms: body weight loss > 20%, watery diarrhea, and glossy bleeding. Results are expressed as mean \pm SEM. * p < 0.05 VS Control. **c** Colon length at necropsy. Results are expressed as mean \pm SD. * p < 0.001 VS Control of the same period of induction. **d** and **e** Representative images of the colon length and macroscopic findings at day 4 and day 7, respectively



Effects of DSS on the expression of *Sod1*, *Sod2*, and *Cat* mRNA in the colon

After both day 4 and day 7 of the induction, DSS significantly down-regulated the mRNA expression of antioxidant enzymes *Sod1* (Fig. 6a), *Sod2* (Fig. 6b), and *Cat* (Fig. 6c).

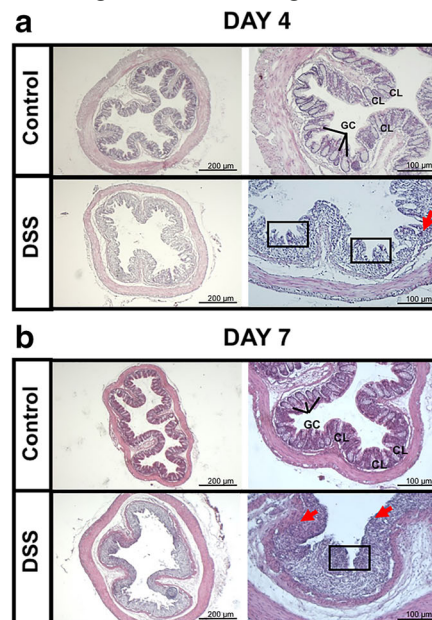
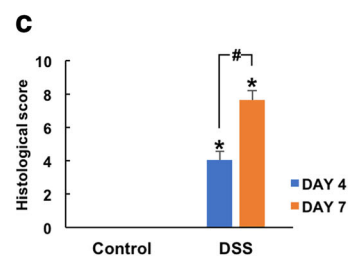


Fig. 2 Effects of DSS on morphology and histological scores of the ICR mouse colon with H&E staining. Representative images of H&E staining of the ICR mouse colonic tissue sections after DSS induction for **a** 4 and **b** 7 days. GC, goblet cells; CL, crypts of Lieberkühn. Red arrows indicate inflammatory cell infiltration; Squares indicate crypt erosion. (C) Histological scores. The score was calculated based on the sum of;

Discussion

After DSS administration UC is characterized macroscopically by colon shortening, edema, and bleeding, and microscopically by damage to the epithelial lining and mucosa, inflammation, and ulceration (Millar et al. 1996;



inflammatory severity (0–3), the extent of inflammation (0–3), and the crypt damage (0–4). A score of 0 indicated normal tissue and a score of 12 indicated the most extensive disease symptoms. Results are expressed as mean \pm SEM. * p < 0.001 VS Control of the same period of induction; # p < 0.05

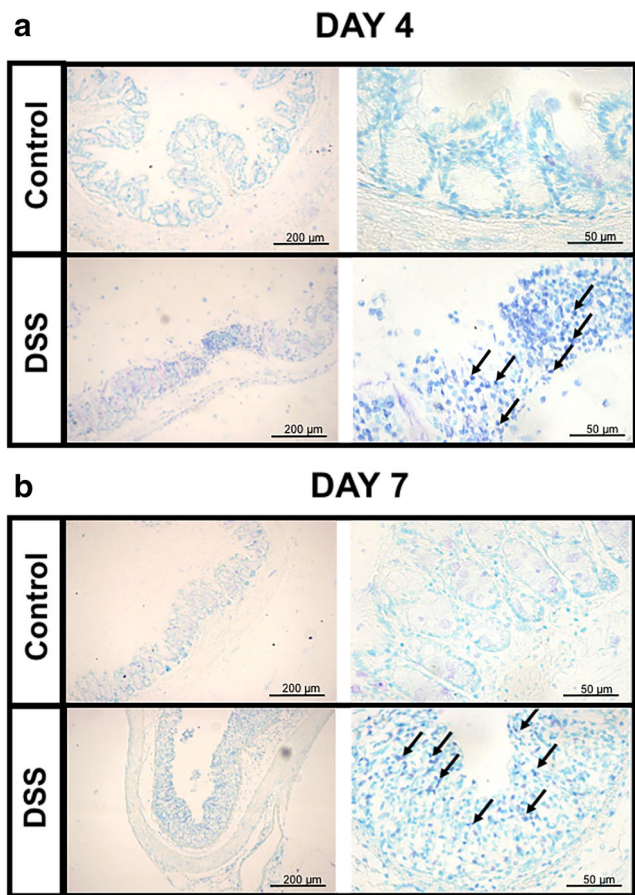


Fig. 3 Histological changes of the DSS-induced ICR mouse colon by toluidine blue staining. Representative images of toluidine blue staining of the ICR mouse colonic tissue sections after DSS induction for **a** 4 and **b** 7 days. Black arrows indicate infiltration of mast cells

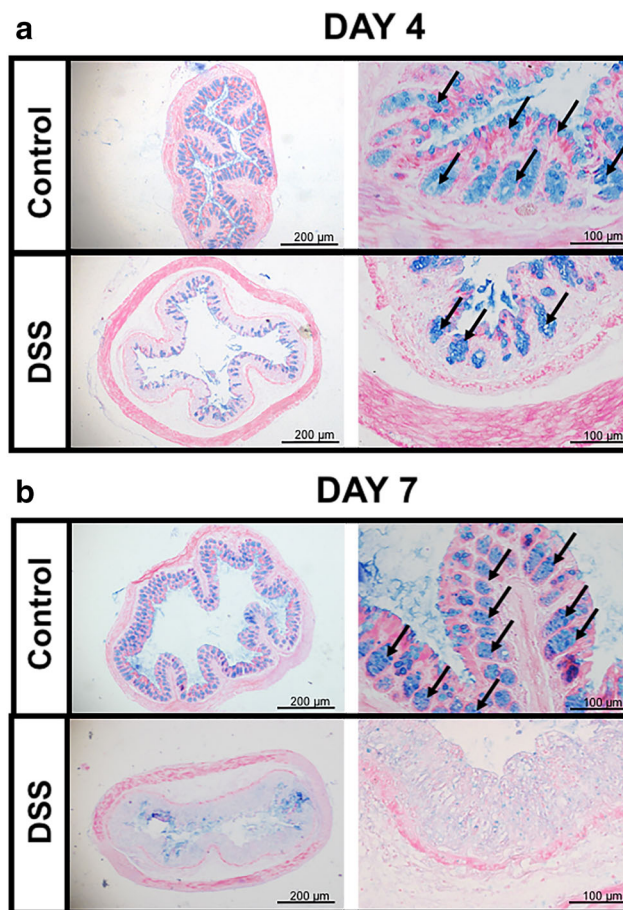


Fig. 4 Histological changes of the DSS-induced ICR mouse colon by alcian blue staining. Representative images of alcian blue staining of the ICR mouse colonic tissue sections after DSS induction for **a** 4 and **b** 7 days. Black arrows indicate mucin

Wallace et al. 1989). Forty kDa DSS was chosen for this study because it has previously been shown to induce severe UC in mice (Perše and Cerar 2012). Lower molecular weight DSS (5 kDa) can induce only mild UC in mice and higher molecular weight DSS (500 kDa) fails to induce UC at all (Perše and Cerar 2012) as it is unable to penetrate the mucosal membrane of the colon (Kitajima et al. 2000).

Most DSS-induced UC murine models have been established in inbred strains such as C57BL/6JRj and BALB/c with 4–7 day-induction-periods (Gutierrez-Orozco et al. 2014; Kang et al. 2017; Mahler et al. 1998; Melgar et al. 2005; Xiao et al. 2013) while DSS-induced UC models in outbred mouse strains, which represent population genetic diversity, are very limited (Perše and Cerar 2012) with prolonged 7–12 day induction-periods (Fang et al. 2013; Seo et al. 2017). DSS-induced UC models in ICR mice have used variable DSS concentrations and induction-periods (Perše and Cerar 2012). Our DSS-induced UC model in ICR mice used a minimal amount of DSS and a short induction-period (DSS 6 g/kg/day for 4 consecutive days).

In the study of Akiyama et al. (2012), UC was induced in male ICR mice (5-week-old) by administration of 3% DSS in drinking water for 2 weeks. Hong et al. (2019) and Kim et al.

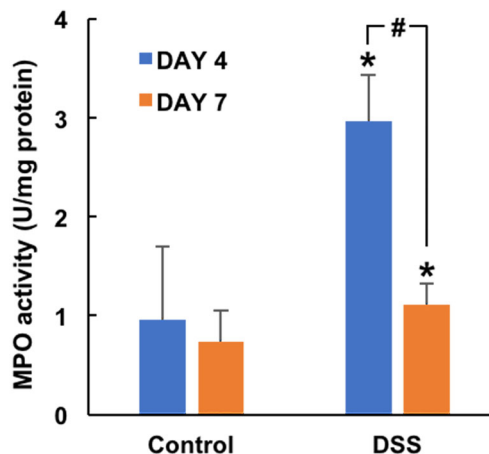


Fig. 5 Effects of DSS on myeloperoxidase (MPO) activity in the ICR mouse colons. The ICR mice were induced by DSS for 4 or 7 days. After the last treatment, MPO activity was examined in the colonic tissues. Results are expressed as mean \pm SD. * $p < 0.05$ VS Control; # $p < 0.001$

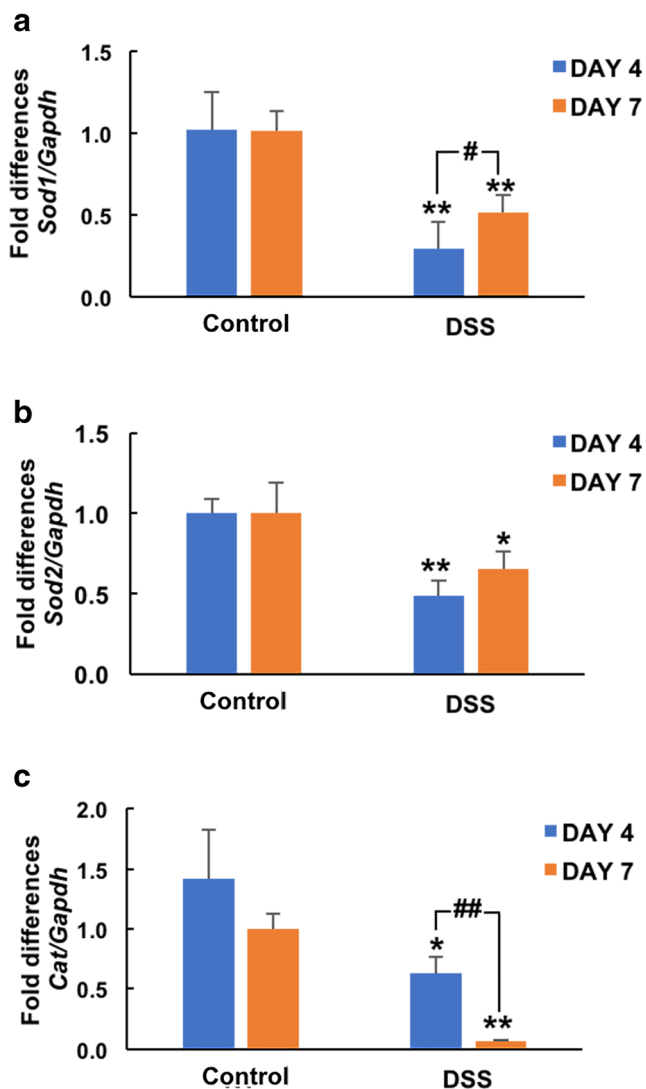


Fig. 6 Effects of DSS on the expression of *Sod1*, *Sod2*, and *Cat* mRNA in the ICR mouse colons. The ICR mice were induced by DSS for 4 or 7 days. After the last treatment, the expression of **a** *Sod1*, **b** *Sod2*, and **c** *Cat* mRNA were quantitatively determined in the colonic tissues by RT/q-PCR. Results are expressed as mean±SD. * $p < 0.05$ and ** $p < 0.001$ VS Control; # $p < 0.05$ and ## $p < 0.001$.

(2020) induced UC in male ICR mice (5-week-old) with 4% DSS in drinking water for 9 days. Kawabata et al. (2006) induced UC in female ICR mice (5-week-old) with 3% DSS in drinking water for 7 days and Seo et al. (2017) induced UC in male ICR mice (weighing 28–30 g) with drinking water containing 3% DSS for 12 days. Finally, Cho et al. (2011) used 5% DSS in drinking water for 7 days to induce UC in male ICR mice. A previous study reported that outbred mice treated with DSS developed lesions in the middle colon followed by the distal colon (Murthy and Flanigan 1999), while inbred mice developed lesions in the proximal colon followed by the distal colon. Interestingly, in our model, the DSS-induced inflammation extended for the whole colon, including cecum. In the present study, macroscopic and

histopathological findings indicate that DSS efficiently induced UC in ICR mice within 4 days. In our model, after 4 days, increased DAI scores were achieved with associated diarrhea, hematochezia, colon edema and shortening, followed by infiltration of inflammatory cells to the colon, accumulation of mast cells in the mucosa, goblet cell loss, mucin depletion, crypt damage, and epithelial erosion. Evaluation of DSS-induced UC has utilized both histological and functional scores to determine the disease severity (Mosli et al. 2017; Nishiyama et al. 2012). The results from our model show a significant increase in histological scores in the DSS-treated mice compared to the non-treated mice. We also demonstrated a shorter optimal induction period of DSS-induced UC in ICR mice by using a precise DSS dosage regimen. The mice in our model were intergastrically administered 0.25 mL of 21% DSS by gastric lavage-tube 4 times per day. We saw UC symptoms in the mice and increased DAI and histological scores after 4 days. Therefore, this model represents an acute UC model that could be useful for searching or screening new anti-inflammatory or antioxidant compounds to help protect the colon in UC therapy.

Though the mechanism of DSS-induced UC has not been clearly elucidated, there are reports that DSS-induced UC is associated with inflammatory responses through oxidative stress triggering (Bhattacharyya et al. 2009; Damiani et al. 2007). Oxidative stress is one of the significant factors in UC pathogenesis. The overproduction of reactive oxygen species (ROS) can trigger an immune response in the colon (Yao et al. 2010) and cause tissue injury via activation and proliferation of inflammatory and epithelial cells (Kruidenier and Verspaget 2002). The present study reveals an oxidant-antioxidant imbalance in DSS-induced UC in ICR mice via a significant down-regulation of *Sod1*, *Sod2* and *Cat* mRNA with a concomitant increase in MPO activity. These findings indicate that the enzymatic antioxidant system is likely to be an indirect UC trigger.

In the oxidative stress pathway, antioxidant enzymes perform a critical function in neutralizing free radicals; however, the enzymatic defense system might be overwhelmed during inflammation (Pavlick et al. 2002). It has been noted that UC patients exhibit impaired mucosal antioxidant defenses in inflamed tissues (Buffinton and Doe 1995) with lower levels of SOD (Ishihara et al. 2009; Mulder et al. 1991). In rats, the serum levels of SOD and CAT were drastically reduced after administration of 3 and 5% DSS (5 kDa) for 7 days (Pengkumsri et al. 2015). In addition, levels of SOD and CAT enzymes in mouse colonic tissues decrease after receiving 2% DSS (35–50 kDa) for 6 days (Kim et al. 2010). In the present study, the DSS impaired oxidant-antioxidant balance in the colon was seen through the significant decline in the expression of *Sod1*, *Sod2*, and *Cat* mRNA, three genes encoding pivotal antioxidant enzymes. SOD is the first defensive enzyme against free radicals, transforming superoxide

anion into hydrogen peroxide, which is then turned to water and oxygen by CAT (Pavlick et al. 2002). SODs are categorized into copper-zinc SOD (Cu/Zn-SOD or SOD1), which is abundant in the cytosol, and manganese SOD (Mn-SOD or SOD2), which is commonly found in mitochondria and peroxisomes (Guan and Lan 2018). CAT primarily located in peroxisomes plays a critical role in catalyzing the reduction of hydrogen peroxide thereby preventing the harmful effects of oxidative radicals (Guan and Lan 2018; Pervin et al. 2016).

Neutrophils play a crucial role in intestinal homeostasis and the accumulation of neutrophils in the inflamed mucosal tissues is a prominent feature of UC (Masoodi et al. 2011). Infiltration of neutrophils in the intestinal mucosa and the crypts is directly associated with the epithelial disruption seen in UC (Naito et al. 2007). Neutrophils have granules that contain numerous enzymes, including MPO, which is considered a biomarker of neutrophil accumulation in inflamed areas (Ribeiro et al. 2011). In mice, neutrophils can have a very short half-life (8–10 h) when labeled *in vivo* (Basu et al. 2002). However, neutrophils have also been shown to circulate in the blood of mixed C57BL/6 and 129/OLA mice for 96 h, with a 4-fold-drop in numbers after 120 h (Basu et al. 2002). Thus, the calculated blood circulation times of neutrophils can vary from 10 h to over 5 days (Bekkering and Torensma 2013) and our observation of lower levels of MPO on day 7 than on day 4 might be explained by the lifespan of the neutrophils in our model. Therefore, the measurement of MPO activity at day 4 might be a more accurate indication of the neutrophil response in our DSS-induced UC model than at day 7.

Oxidative stress also plays a role in inflammation via activation of neutrophils to produce reactive nitrogen and oxygen species, which aggravate epithelial injury and mucosal damage (Ribeiro et al. 2011). Thus, DSS simultaneously suppressed expression of *Sod1*, *Sod2*, and *Cat* antioxidant genes and increased MPO activity in the inflamed colon via increased infiltration of mast and other inflammatory cells to the mucosal layer.

In the present study, DSS efficiently induced UC in ICR mice within 4 days. There were significant increases in the DAI and histological scores with associated colon shortening, followed by infiltration of mast cells, depletion of goblet cells and mucin, and crypt erosion. MPO activity was increased in DSS-induced colon tissues and expression of *Sod1*, *Sod2*, and *Cat* were all suppressed. Prolonged DSS induction for 7 days increased the severity of UC features at macroscopic, histological, and anti-oxidant levels.

Conclusions

DSS-induced UC in an outbred ICR mouse model was achieved. The model substantiates the pro-oxidant potential of DSS to ultimately provoke UC via the down-regulation of

Sod1, *Sod2*, and *Cat* mRNA expression with a concomitant increase in MPO activity. This model may prove useful for investigating the underlying pathophysiological mechanisms of UC in terms of oxidant-antioxidant balance and for evaluating the efficacy of new therapeutics.

Acknowledgements Nitima Tatiya-aphiradee acknowledges the Royal Golden Jubilee Ph.D. program, Thailand Research Fund for the scholarship (PhD0008/2559). The authors thank Dr. Glenn Borlace, Faculty of Pharmaceutical Sciences, Khon Kaen University for English language assistance.

Author contributions All the authors have accepted responsibility for the entire content of this submitted manuscript and approved the submission.

Compliance with ethical standards

Employment of leadership None declared.

Honorarium None declared.

Conflict of interest The funding organization(s) played no role in the study design; in the collection, analysis, and interpretation of data; in the writing of the report; or in the decision to submit the report for publication.

References

- Akiyama S, Nesumi A, Maeda-Yamamoto M, Uehara M, Murakami A (2012) Effects of anthocyanin-rich tea “Sunrouge” on dextran sodium sulfate-induced colitis in mice. *BioFactors* 38(3):226–233. <https://doi.org/10.1002/biof.1008>
- Balmus IM, Ciobica A, Trifan A, Stanciu C (2016) The implications of oxidative stress and antioxidant therapies in inflammatory bowel disease: clinical aspects and animal models. *Saudi J Gastroenterol* 22:3–17. <https://doi.org/10.4103/1319-3767.173753>
- Barone M, Chain F, Sokol H, Brigidi P, Bermúdez-Humarán LG, Langella P, Martin R (2018) A Versatile new model of chemically induced chronic colitis using an outbred murine strain. *Front Microbiol* 9:565. <https://doi.org/10.3389/fmicb.2018.00565>
- Basu S, Hodgson G, Katz M, Dunn AR (2002) Evaluation of role of G-CSF in the production, survival, and release of neutrophils from bone marrow into circulation. *Blood* 100:854–861. <https://doi.org/10.1182/blood.V100.3.854>
- Baumgart DC, Sandborn WJ (2007) Inflammatory bowel disease: clinical aspects and established and evolving therapies. *Lancet* 369:1641–1657. [https://doi.org/10.1016/S0140-6736\(07\)60751-X](https://doi.org/10.1016/S0140-6736(07)60751-X)
- Bekkering S, Torensma R (2013) Another look at the life of a neutrophil. *World J Hematol* 2(2):44–58. <https://doi.org/10.5315/wjh.v2.i2.44>
- Bhattacharyya S, Dudeja PK, Tobacman JK (2009) ROS, Hsp27, and IKK β mediate dextran sodium sulfate (DSS) activation of IkBa, NFkB, and IL-8. *Inflamm Bowel Dis* 15(5):673–683. <https://doi.org/10.1002/ibd.20821>
- Bradford MM (1976) A rapid and sensitive method for the quantitation of microgram quantities of protein utilizing the principle of protein-dye binding. *Anal Biochem* 72:248–254. [https://doi.org/10.1016/0003-2697\(76\)90527-3](https://doi.org/10.1016/0003-2697(76)90527-3)
- Buffinton GD, Doe WF (1995) Depleted mucosal antioxidant defences in inflammatory bowel disease. *Free Radic Biol Med* 19(6):911–918. [https://doi.org/10.1016/0891-5849\(95\)94362-H](https://doi.org/10.1016/0891-5849(95)94362-H)

- Chassaing B, Aitken JD, Malleshappa M, Vijay-Kumar M (2014) Dextran sulfate sodium (DSS)-induced colitis in mice. *Curr Protoc Immunol* 104(1):15–25. <https://doi.org/10.1002/0471142735.im1525s104>
- Cheon JH, Kim JS, Kim JM, Kim N, Jung HC, Song IS (2006) Plant sterol guggulsterone inhibits nuclear factor-kappaB signaling in intestinal epithelial cells by blocking IkappaB kinase and ameliorates acute murine colitis. *Inflamm Bowel Dis* 12(12):1152–1161. <https://doi.org/10.1097/01.mib.0000235830.94057.c6>
- Cho E, Shin JS, Noh YS, Cho YW, Hong SJ, Park JH, Lee JY, Lee JY, Lee KT (2011) Anti-inflammatory effects of methanol extract of *Patrinia scabiosaefolia* in mice with ulcerative colitis. *J Ethnopharmacol* 136(3):428–435. <https://doi.org/10.1016/j.jep.2010.04.047>
- Damiani CR, Benetton CA, Stoffel C, Bardini KC, Cardoso VH, Di Giunta G, Pinho RA, Dal-Pizzol F, Streck EL (2007) Oxidative stress and metabolism in animal model of colitis induced by dextran sulfate sodium. *J Gastroenterol Hepatol* 22(11):1846–1851. <https://doi.org/10.1111/j.1440-1746.2007.04890.x>
- Fang J, Seki T, Tsukamoto T, Qin H, Yin H, Liao L, Nakamura H, Maeda H (2013) Protection from inflammatory bowel disease and colitis-associated carcinogenesis with 4-vinyl-2, 6-dimethoxyphenol (canolol) involves suppression of oxidative stress and inflammatory cytokines. *Carcinogenesis* 34(12):2833–2841. <https://doi.org/10.1093/carcin/bgt309>
- Frazer KA, Murray SS, Schork NJ, Topol EJ (2009) Human genetic variation and its contribution to complex traits. *Nat Rev Genet* 10(4):241–251. <https://doi.org/10.1038/nrg2554>
- Guan G, Lan S (2018) Implications of antioxidant systems in inflammatory bowel disease. *Biomed Res Int* 2018:1290179. <https://doi.org/10.1155/2018/1290179>
- Gutierrez-Orozco F, Thomas-Ahner JM, Berman-Booty LD, Galley JD, Chitchumroonchokchai C, Mace T, Suksamram S, Bailey MT, Clinton SK, Lesinski GB, Failla ML (2014) Dietary α -mangostin, a xanthone from mangosteen fruit, exacerbates experimental colitis and promotes dysbiosis in mice. *Mol Nutr Food Res* 58(6):1226–1238. <https://doi.org/10.1002/mnfr.201300771>
- Halliwell B (1997) Antioxidants and human disease: a general introduction. *Nutr Rev* 55:S44–S52. <https://doi.org/10.1111/j.1753-4887.1997.tb06100.x>
- Hirata I, Yasumoto S, Toshina K, Inoue T, Nisigikawa T, Murano N, Murano M, Wang FY, Katsu K (2007) Evaluation of the effect of pyrrolidine dithiocarbamate in suppressing inflammation in mice with dextran sodium sulfate-induced colitis. *World J Gastroenterol* 13(11):1666–1671. <https://doi.org/10.3748/wjg.v13.i11.1666>
- Hong J, Chung KS, Shin JS, Park G, Jang Y, Lee KT (2019) Anti-colitic effects of ethanol extract of *Persea americana* Mill. through suppression of pro-inflammatory mediators via NF- κ B/STAT3 inactivation in dextran sulfate sodium-induced colitis mice. *Int J Mol Sci* 20(1):E177. <https://doi.org/10.3390/ijms20010177>
- Ishihara T, Tanaka K, Tasaka Y, Namba T, Suzuki J, Ishihara T, Okamoto S, Hibi T, Takenaga M, Igarashi R, Sato K, Mizushima Y, Mizushima T (2009) Therapeutic effect of lecithinized superoxide dismutase against colitis. *J Pharmacol Exp Ther* 328(1):152–164. <https://doi.org/10.1124/jpet.108.144451>
- Jarukamjorn K, Sakuma T, Miyaura J, Nemoto N (1999) Different regulation of the expression of mouse hepatic cytochrome P450 2B enzymes by glucocorticoid and phenobarbital. *Arch Biochem Biophys* 369(1):89–99. <https://doi.org/10.1006/abbi.1999.1342>
- Jarukamjorn K, Chatuphonprasert W, Jearapong N, Punvittayagul C, Wongpoomchai R (2019) Tetrahydrocurcumin attenuates phase I metabolizing enzyme-triggered oxidative stress in mice fed a high-fat and high-fructose diet. *J Func Food* 55:117–125. <https://doi.org/10.1016/j.jff.2019.02.021>
- Kang Y, Xue Y, Du M, Zhu MJ (2017) Preventive effects of Goji berry on dextran-sulfate-sodium-induced colitis in mice. *J Nutr Biochem* 40:70–76. <https://doi.org/10.1016/j.jnutbio.2016.10.009>
- Kawabata K, Murakami A, Ohigashi H (2006) Auraptene decreases the activity of matrix metalloproteinases in dextran sulfate sodium-induced ulcerative colitis in ICR mice. *Biosci Biotechnol Biochem* 70(12):3062–3065. <https://doi.org/10.1271/bbb.60393>
- Kim M, Murakami A, Miyamoto S, Tanaka T, Ohigashi H (2010) The modifying effects of green tea polyphenols on acute colitis and inflammation-associated colon carcinogenesis in male ICR mice. *Biofactors* 36(1):43–51. <https://doi.org/10.1002/biof.69>
- Kim JJ, Shajib MS, Manocha MM, Khan WI (2012) Investigating intestinal inflammation in DSS-induced model of IBD. *J Vis Exp* 60:1–6. <https://doi.org/10.3791/3678>
- Kim JE, Nam JH, Cho JY, Kim KS, Hwang DY (2017) Annual tendency of research papers used ICR mice as experimental animals in biomedical research fields. *Lab Anim Res* 33(2):171–178. <https://doi.org/10.5625/lar.2017.33.2.171>
- Kim M, Chung KS, Hwang SJ, Yoon YS, Jang YP, Lee JK, Lee KT (2020) Protective effect of *Cicer arietinum* L. (chickpea) ethanol extract in the dextran sulfate sodium-induced mouse model of ulcerative colitis. *Nutrients* 12(2):E456. <https://doi.org/10.3390/nu12020456>
- Kitajima S, Takuma S, Morimoto S (2000) Histological analysis of murine colitis induced by dextran sulfate sodium of different molecular weights. *Exper Anim* 49(1):9–15. <https://doi.org/10.1538/expanim.49.9>
- Kruidenier L, Verspaget HW (2002) Review article: oxidative stress as a pathogenic factor in inflammatory bowel disease—radicals or ridiculous? *Aliment Pharmacol Ther* 16:1997–2015. <https://doi.org/10.1046/j.1365-2036.2002.01378.x>
- Mahler M, Bristol IJ, Leiter EH, Workman AE, Birkenmeier EH, Elson CO, Sundberg JP (1998) Differential susceptibility of inbred mouse strains to dextran sulfate sodium-induced colitis. *Am J Physiol* 274(3):G544–G551. <https://doi.org/10.1152/ajpgi.1998.274.3.G544>
- Masoodi I, Tijjani BM, Wani H, Hassan NS, Khan AB, Hussain S (2011) Biomarkers in the management of ulcerative colitis: a brief review. *Ger Med Sci* 9:Doc03. <https://doi.org/10.3205/000126>
- Melgar S, Karlsson A, Michaëlsson E (2005) Acute colitis induced by dextran sulfate sodium progresses to chronicity in C57BL/6 but not in BALB/c mice: correlation between symptoms and inflammation. *Am J Physiol Gastrointest Liver Physiol* 288(6):G1328–G1338. <https://doi.org/10.1152/ajpgi.00467.2004>
- Millar AD, Rampton DS, Chander CL, Claxson AW, Blades S, Coumbe A, Panetta J, Morris CJ, Blake DR (1996) Evaluating the antioxidant potential of new treatments for inflammatory bowel disease in a rat model of colitis. *Gut* 39:407–415. <https://doi.org/10.1136/gut.39.3.407>
- Mosli MH, Parker CE, Nelson SA, Baker KA, MacDonald JK, Zou GY, Feagan BG, Khanna R, Levesque BG, Jairath V (2017) Histologic scoring indices for evaluation of disease activity in ulcerative colitis. *Cochrane Database Syst Rev* 25(5):CD011256. <https://doi.org/10.1002/14651858.CD011256.pub2>
- Mulder TP, Verspaget HW, Janssens AR, de Bruin PA, Peña AS, Lamers CB (1991) Decrease in two intestinal copper/zinc containing proteins with antioxidant function in inflammatory bowel disease. *Gut* 32(10):1146–1150. <https://doi.org/10.1136/gut.32.10.1146>
- Murthy S, Flanigan A (1999) Animal models of inflammatory bowel disease. In: Morgan DW, Marshall LA (eds) *In vivo* models of inflammation. Birkhäuser, Basel, pp 205–236
- Naito Y, Takagi T, Yoshikawa T (2007) Neutrophil-dependent oxidative stress in ulcerative colitis. *J Clin Biochem Nutr* 41:18–36. <https://doi.org/10.3164/jcbs.2007003>
- Nishiyama Y, Kataoka T, Yamato K, Taguchi T, Yamaoka K (2012) Suppression of dextran sulfate sodium-induced colitis in mice by

- radon inhalation. *Mediat Inflamm* 2012:239617. <https://doi.org/10.1155/2012/239617>
- Ordás I, Eckmann L, Talamini M, Baumgart DC, Sandborn WJ (2012) Ulcerative colitis. *Lancet* 380(9853):1606–1619. [https://doi.org/10.1016/S0140-6736\(12\)60150-0](https://doi.org/10.1016/S0140-6736(12)60150-0)
- Pavlick KP, Laroux FS, Fuseler J, Wolf RE, Gray L, Hoffman J, Grisham MB (2002) Role of reactive metabolites of oxygen and nitrogen in inflammatory bowel disease. *Free Radic Biol Med* 33(3):311–322. [https://doi.org/10.1016/S0891-5849\(02\)00853-5](https://doi.org/10.1016/S0891-5849(02)00853-5)
- Pengkumsri N, Suwannalert P, Sivamaruthi BS, Wongpoomchai R, Sirisattha S, Tammasakchai A, Taya S, Sirilun S, Peerajan S, Chaiyasut C (2015) Molecular, histological, and anti-oxidant evaluation of colitis induction in rats by different concentration of dextran sodium sulfate (5 kDa). *Int J Pharm Sci* 7(12):283–287. <https://innovareacademics.in/journals/index.php/ijpps/article/view/9356>
- Perše M, Cerar A (2012) Dextran sodium sulphate colitis mouse model: traps and tricks. *J Biomed Biotechnol* 2012:10–12. <https://doi.org/10.1155/2012/718617>
- Pervin M, Hasnat A, Lim JH, Lee YM, Eun Kim O, Um BH, Lim BO (2016) Preventive and therapeutic effects of Blueberry (*Vaccinium corymbosum*) extract against DSS-induced ulcerative colitis by regulation of antioxidant and inflammatory mediators. *J Nutr Biochem* 28:103–113. <https://doi.org/10.1016/j.jnutbio.2015.10.006>
- Ribeiro AL, Shimada AL, Hebeda CB, de Oliveira TF, de Melo Loureiro AP, Filho Wdos R, Santos AM, de Lima WT, Farsky SH (2011) *In vivo* hydroquinone exposure alters circulating neutrophil activities and impairs LPS-induced lung inflammation in mice. *Toxicology* 288(1–3):1–7. <https://doi.org/10.1016/j.tox.2011.05.009>
- Seo S, Shin JS, Lee WS, Rhee YK, Cho CW, Hong HD, Lee KT (2017) Anti-colitis effect of *Lactobacillus sakei* K040706 via suppression of inflammatory responses in the dextran sulfate sodium-induced colitis mice model. *J Func Foods* 27:256–268. <https://doi.org/10.1016/j.jff.2016.12.045>
- Singh S, Graff LA, Bernstein CN (2009) Do NSAIDs, antibiotics, infections, or stress trigger flares in IBD? *Am J Gastroenterol* 104(5):1298–1313. <https://doi.org/10.1038/ajg.2009.15>
- Stevceva L, Pavli P, Buffinton G, Wozniak A, Doe WF (1999) Dextran sodium sulphate-induced colitis activity varies with mouse strain but develops in lipopolysaccharide-unresponsive mice. *J Gastroenterol Hepatol* 14(1):54–60. <https://doi.org/10.1046/j.1440-1746.1999.01806.x>
- Tamaki H, Nakamura H, Nishio A, Nakase H, Ueno S, Uza N, Kido M, Inoue S, Mikami S, Asada M, Kiriya K, Kitamura H, Ohashi S, Fukui T, Kawasaki K, Matsuura M, Ishii Y, Okazaki K, Yodoi J, Chiba T (2006) Human thioredoxin-1 ameliorates experimental murine colitis in association with suppressed macrophage inhibitory factor production. *Gastroenterology* 131(4):1110–1121. <https://doi.org/10.1053/j.gastro.2006.08.023>
- Tatiya-aphiradee N, Chatuphonprasert W, Jarukamjorn K (2019) Anti-inflammatory effect of *Garcinia mangostana* Linn. pericarp extract in methicillin-resistant *Staphylococcus aureus*-induced superficial skin infection in mice. *Biomed Pharmacother* 111:705–713. <https://doi.org/10.1016/j.biopha.2018.12.142>
- Wallace JL, MacNaughton WK, Morris GP, Bech PL (1989) Inhibition of leukotriene synthesis markedly accelerates healing in a rat model of inflammatory bowel disease. *Gastroenterology* 96(1):26–36. [https://doi.org/10.1016/0016-5085\(89\)90760-9](https://doi.org/10.1016/0016-5085(89)90760-9)
- Xavier RJ, Podolsky DK (2007) Unravelling the pathogenesis of inflammatory bowel disease. *Nature* 448(7152):427–434. <https://doi.org/10.1038/nature06005>
- Xiao HT, Lin Cy, Ho DH, Peng J, Chen Y, Tsang SW, Wong M, Zhang XJ, Zhang M, Bian ZX (2013) Inhibitory effect of the gallotannin corilagin on dextran sulfate sodium-induced murine ulcerative colitis. *J Nat Prod* 76(11):2120–2125. <https://doi.org/10.1021/np4006772>
- Yao J, Wang JY, Liu L, Li YX, Xun AY, Zeng WS, Jia CH, Wei XX, Feng JL, Zhao L, Wang LS (2010) Anti-oxidant effects of resveratrol on mice with DSS-induced ulcerative colitis. *Arch Med Res* 41(4):288–294. <https://doi.org/10.1016/j.arcmed.2010.05.002>